9106 *Biochemistry* **2010,** *49,* 9106–9112
DOI: 10.1021/bi1009503

BIOCHEMISTRY
including biophysical chemistry & molecular biology
Article

Combinatorial Selection of DNA Thioaptamers Targeted to the HA Binding Domain of Human CD44[†]

Anoma Somasunderam,[‡,§] Varatharasa Thiviyanathan,[‡] Takemi Tanaka,[§,⊥] Xin Li,[‡] Muniasamy Neerathilingam,[‡] Ganesh Lakshmana Rao Lokesh,[‡] Aman Mann,[§] Yang Peng,[§] Mauro Ferrari,[§,⊥,∥,@] Jim Klostergaard,*[,▽] and David G. Gorenstein*[,‡,§]

[‡]*Institute of Molecular Medicine,* [§]*Department of Nanomedicine and Biomedical Engineering, University of Texas Health Science Center, Houston, Texas 77030, United States,* [∥]*Department of Bioengineering, Rice University, Houston, Texas 77005, United States,* [⊥]*Department of Biomedical Engineering, University of Texas, Austin, Texas 78712, United States,* [@]*Department of Experimental Therapeutics, and* [▽]*Department of Molecular and Cellular Oncology, University of Texas M. D. Anderson Cancer Center, Houston, Texas 77030, United States*

Received June 13, 2010; Revised Manuscript Received September 8, 2010

ABSTRACT: CD44, the primary receptor for hyaluronic acid, plays an important role in tumor growth and metastasis. CD44−hyaluronic acid interactions can be exploited for targeted delivery of anticancer agents specifically to cancer cells. Although various splicing variants of CD44 are expressed on the plasma membrane of cancer cells, the hyaluronic acid binding domain (HABD) is highly conserved among the CD44 splicing variants. Using a novel two-step process, we have identified monothiophosphate-modified aptamers (thioaptamers) that specifically bind to the CD44's HABD with high affinities. Binding affinities of the selected thioaptamers for the HABD were in the range of 180−295 nM, an affinity significantly higher than that of hyaluronic acid (K_d above the micromolar range). The selected thioaptamers bound to CD44 positive human ovarian cancer cell lines (SKOV3, IGROV, and A2780) but failed to bind the CD44 negative NIH3T3 cell line. Our results indicated that thio substitution at specific positions of the DNA phosphate backbone results in specific and high-affinity binding of thioaptamers to CD44. The selected thioaptamers will be of great interest for further development as a targeting or imaging agent for the delivery of therapeutic payloads for cancer tissues.

The CD44 proteoglycan family of transmembrane glycoproteins is ubiquitously expressed in physiological and pathological systems (*1*). Studies of tumorigenesis using CD44 antibodies and vaccines have shown the importance of CD44 in tumor growth and metastasis (*2*, *3*). CD44 is the primary cell surface receptor for hyaluronic acid (HA),[1] binding this ligand via a Link module, a lectin-like fold (*4*, *5*). The HA binding domain (HABD) is stabilized by three disulfide bridges and is centered around the N-terminal Link module in the extracellular domain of CD44 but extends beyond the Link involving additional basic residues. The Link module is highly conserved among CD44 family members and has only two disulfide bridges. The solution and crystal structures of the HABD are available (*6*−*8*). Although CD44 is encoded by a single gene, numerous transcripts are formed by alternative splicing. Standard CD44 (CD44S) is comprised of the constant, nonvariant exon products, whereas the variant isoforms arise by splicing of additional exon products into a single site within the membrane-proximal region of the ectodomain. Carcinomas typically produce several CD44 variants as well as decreased proportions of CD44S, and many studies have implicated CD44 variants rather than CD44S in tumor progression (*9*, *10*). CD44 requires "activation" with respect to HA binding and consequent signaling, possibly through localization of CD44 within specialized plasma membrane lipid microdomains or rafts, from which endocytosis of HA and CD44 occurs (*11*).

CD44 is increasingly recognized as a marker for subpopulations of tumor-initiating cells or cancer stem cells (CSCs), which are highly malignant and chemoresistant, likely because of increased anti-apoptotic pathway activity and enrichment of multidrug transporters (*12*). Epithelial−mesenchymal transition (EMT) has been linked to the properties of CD44 positive (CD44+) and CD24 negative CSCs, as well as to HA (*13*). There is a growing body of evidence of HA-dependent association of CD44 with receptor tyrosine kinases and transporters, important in drug resistance and malignancy (*14*). Recent studies of the CD44+ CSC-like subpopulation of cells isolated from human patient epithelial ovarian carcinoma specimens and ascites revealed that the CSCs are enriched with ABC family drug transporters, ABCG2/BCRP1 and MDR1, as well as activated TLR4/MyD88 and NF-κB (*15*−*17*). These mechanisms may account for the drug resistance of CSC, a critical aspect of their phenotype and importance in therapeutic response. HA−CD44 interactions can be exploited for the delivery of chemotherapeutic drugs and other anticancer agents to cancer cells. Many investigators have shown increased efficacy in cell and animal tumor models by conjugating drugs to HA or

[†]This work was supported by the National Institutes of Health (GM084552, N01-HV28184, CC987654321, R01CA128797, and 2U54CA096300-06A1), the Department of Defense (W81XWH-07-2-0101 and W81XWH-09-1-0212), the Welch Foundation (H-1296), and the Alliance for Nano Health.

*To whom correspondence should be addressed. J.K.: Department of Molecular and Cellular Oncology, University of Texas M. D. Anderson Cancer Center, 1515 Holcombe Blvd., Houston, TX 77030; e-mail, jkloster@mdanderson.org; phone, (713) 792-8962; fax, (713) 794-3270. D.G.G.: Institute of Molecular Medicine, University of Texas Health Science Center, 1825 Pressler, Houston, TX 77030; e-mail, david.g.gorenstein@uth.tmc.edu; phone, (713) 500-2233; fax, (713) 500-2420.

[1]Abbreviations: HA, hyaluronic acid; HABD, hyaluronic acid binding domain; HABP, hyaluronic acid binding protein; IgG, immunoglobulin G; dNTP, deoxynucleotide triphosphate; TA, thioaptamer.

 Published on Web 09/15/2010

anti-CD44 antibodies, as well as incorporating drugs or siRNAs into vehicles that have been decorated with HA or antibodies (*18*, *19*). Further selective targeting to tumor-relevant and overexpressed variants of CD44 is a substantial goal. However, there is evidence that HA interactions with the CD44 splice variants are weakened compared to those with CD44S (*20*), contrary to this goal. Thus, the use of aptamer technology to develop a library of high-affinity and individually specific CD44S and CD44 splice-variant aptamers is a significant first step in achieving this level of refined targeting.

Aptamers are small, structurally distinct oligonucleotide molecules that exhibit specific and high binding affinities for proteins and other biological macromolecules. Aptamers are emerging as attractive alternatives over conventional ligands such as antibodies and peptides for diagnostic and therapeutic applications (*21*−*24*). Aptamers can be obtained through an in vitro selection process (*25*, *26*) against virtually any kind of molecule, whereas antibodies generally require biological systems that must be induced by an immune response. Compared to antibodies, the smaller size of aptamers makes them easier to synthesize in large quantities and makes it easier to introduce a wide range of chemical modifications. Through chemical modifications, the kinetic parameters and binding affinities can be modified for the aptamers (*27*). Aptamers, in general, exhibit a longer shelf life and are easy to store.

Native oligonucleotides are susceptible to digestion by cellular nucleases, but sugar−phosphate backbone modifications can render them more resistant to degradation (*28*, *29*). Among the several modifications reported over the past two decades, the sulfur substitution of the phosphate backbone is the most commonly performed (*29*). Thioaptamers are backbone-modified aptamers in which one (monothio) or both (dithio) of the nonbridging phosphoryl oxygens are substituted with sulfur. Because sulfur substitution often increases the binding affinity of the oligonucleotide for the protein (*30*, *31*), complete substitution of the phosphate backbone might lead to nonspecific binding of the selected aptamer. A novel method developed in our laboratory (*32*, *33*) allows us to optimize both the number and position of the thio substitutions in the DNA aptamer sequence.

Using combinatorial selection methods, a strategy for identifying nucleotide sequences with high affinity for the target protein, we have selected DNA thioaptamers that specifically bind to the HABD of CD44. In this paper, we report the selection, binding, and cell-based assays of the thioaptamers selected against the HABD of CD44.

MATERIALS AND METHODS

Materials. Cell-free recombinant protein expression kits (RTS500HY) containing *Escherichia coli* lysates were obtained from Roche Diagnostics (Indianapolis, IN). The CD44−HABD construct (CD44−HABD), cloned into the pET19b vector, was obtained from Genescript Inc. (Piscataway, NJ). Templates for DNA synthesis were obtained from Midland Certified Reagents (Midland, TX). Taq polymerase and the chirally pure S_p isomer of dATP(αS) were obtained from Axxora LLC (San Diego, CA). Magnetic (MPG) Streptavidin beads, used for the single-strand, biotinylated DNA isolation, were purchased from Pure Biotech (Middlesex, NJ). Recombinant human CD44−Fc chimera (CD44−Fc), containing residues 21−220 of CD44 fused with human IgG (residues 100−330), was obtained from R&D Systems Inc. (Minneapolis, MN). HABP was purchased from EMD Chemicals (Gibbstown, NJ). The CD44 antibody was purchased from Abcam (Cambridge, MA). TOPO TA cloning kits were obtained from Invitrogen (Carlsbad, CA) and the plasmid isolation kits from Qiagen (Foster city, CA). Biotinylated HA was purchased from Sigma (St. Louis, MO).

Cell Lines and Culture. The human epithelial CD44+ ovarian cancer cell lines, SKOV3, IGROV, and A2780, were kind gifts from A. K. Sood (University of Texas M. D. Anderson Cancer Center). The cells were maintained in RPMI-1640 medium supplemented with 15% fetal bovine serum and 0.1% Gentamicin sulfate. The CD44 negative (CD44−) NIH3T3 mouse fibroblast cell line was maintained in Dulbecco's modified Eagle's medium (DMEM) supplemented with 10% fetal bovine serum. All experiments were performed with 70−80% confluent cultures with 5% CO_2 at 37 °C.

Protein Expression and Purification. CD44−HABD (20−178 amino acid residues) was produced by in vitro (cell-free) expression methods using the RTS500HY kit (*E. coli*-based cell-free expression system). DNA encoding residues 20−178 was synthesized and cloned into expression vector pET19b between the NdeI and BamHI sites. A 3 mL reaction mixture was used for the cell-free expression, using the RTS500 HY kit, following procedures described previously (*34*). After incubation for 12 h at 30 °C with gentle agitation, the protein was recovered by centrifugation and refolded and purified following published procedures (*35*). The purity and concentration of the recovered protein were analyzed by analytical gel electrophoresis and UV absorbance, respectively. HA binding to isolated CD44−HABD was confirmed using biotinylated HA. The tertiary structure and the proper folding of CD44−HABD were confirmed by testing with conformation-specific monoclonal antibody F10.44.2 and ^{15}N HSQC NMR spectroscopy (*6*, *7*).

Synthesis of the Thioaptamer Library. The initial library was synthesized from a 73-mer DNA template containing a 30-nucleotide random region flanked by 21-mer and 22-mer polymerase chain reaction (PCR) primer regions. The library was annealed with the reverse primer, subjected to Klenow reaction for 5 h at 37 °C, and amplified by PCR using AmpliTaq DNA polymerase and a mixture of dATP(αS), dTTP, dCTP, and dGTP to give the thio-substituted library. Reaction conditions for the PCR amplifications were as follows: oligonucleotide library (40 nM), dNTP mixture of dATP(αS), dTTP, dCTP, and dGTP (80 μM each), $MgCl_2$ (2 mM), 5′-biotinylated forward primer and reverse primer (300 nM each), and AmpliTaq DNA polymerase (1 unit) in a total volume of 100 μL. PCR was conducted for 35 cycles of 94 °C (2 min), 55 °C (2 min), and 72 °C (2 min). The resulting 73-mer library contained monothiophosphate substitutions (in the S_p configuration) on the 5′ side of every dA residue with the exception of the primer region on the nontemplate strand.

Single-stranded DNA (ssDNA) was isolated from the double-stranded PCR products by the following procedure using the MPG Streptavidin beads. The 5′-biotinylated DNA strands were mixed with MPG Streptavidin beads in buffer containing 10 mM Tris-HCl, 2 M NaCl, and 1 mM EDTA (pH 7.4) and incubated for 30 min. After the magnetic beads bound to oligonucleotides had been washed three times, the melting solution (0.1 M NaOH) was added to remove the nonbiotinylated strand. The solution of ssDNA TA library was pooled, purified, and denatured in binding buffer at 95 °C for 5 min and the reaction quenched on ice. The fluorescein-labeled, single-stranded TA library was synthesized from the PCR of the template with the 5′-biotinylated forward primer and the 5′-fluorescein-labeled reverse primer.

Combinatorial Selection of Thioaptamers. Purified CD44−HABD containing the histidine tag was bound to the nickel-nitrotriacetic acid (Ni-NTA) beads in buffer containing 50 mM Tris-HCl and 50 mM NaCl (pH 7.4). Prior to screening the TA library to select sequences binding CD44−HABD, we excluded the sequences that could bind the Ni-NTA beads from the library by incubating the initial ssDNA library with Ni-NTA beads, in binding buffer [50 mM Tris-HCl and 20 mM $MgCl_2$ (pH 7.4)]. The reaction mixture was spun at 500*g* for 5 min, the supernatant carefully removed, and the unbound TA library in the supernatant used in the selection experiments. This prescreened TA library (200 pmol) in binding buffer [50 mM Tris-HCl and 20 mM $MgCl_2$ (pH 7.4)] was mixed with CD44−HABD protein bound to the Ni-NTA beads (400−100 pmol) and incubated with gentle shaking for 30−60 min. The beads were spun and placed on a magnet, and the supernatant liquid was carefully removed. The TA-bound Ni-NTA beads were washed four times with the binding buffer to remove unbound sequences, and the bound TAs were subsequently eluted with 500 mM imidazole in binding buffer. The eluted TA library was PCR amplified and taken to the next cycle of the iteration. At each iterative cycle, the stringency of binding was increased by gradually decreasing both the amount of protein and incubation time and increasing the number of washes of the TA−protein complex on the beads. All incubations were conducted at room temperature.

Cloning Procedure and Structural Analysis. The selected TA libraries from the 5th and 10th rounds were amplified with a dNTP mixture and unmodified primers, cloned into the pCT2.1 TOPO vector, and transformed into *E. coli* TOPO 10F′ cells. The *E. coli* colonies containing plasmid DNA with single sequences were picked, and the plasmids were isolated using the miniprep kit (Qiagen) and sequenced. A subset of sequences from the initial library, the 5th and 10th selection rounds were determined. The primary sequences obtained from the 10th cycle were analyzed using ClustalW (*36*) (www.ebi.ac.uk/clustalw) and were grouped into six groups based on the convergence of the primary sequence.

Filter Binding Assays. A filter binding assay was used to measure the equilibrium binding constants of selected TAs for both the CD44−Fc chimera and recombinant CD44−HABD. Biotinylated TAs (15 nM) were incubated with varying concentrations of the CD44 proteins (from 20 to 1500 nM) in 3.5 μL of buffer T [10 mM Tris-HCl (pH 7.4)] for 30 min. The dot-blot apparatus (Bio-Rad) was set up with filter pads at the bottom, a nylon membrane in the middle (to trap the uncomplexed TAs), and a nitrocellulose membrane on top (to trap the CD44−TA complex), and all the membranes were wetted with buffer T. After incubation, samples were diluted to 30 μL with buffer T, transferred to the dot-blot apparatus, and filtered under vacuum. The membranes were washed with buffer T (100 μL) three times to wash away any unbound TAs from the nitrocellulose membrane down to the nylon membrane. After the washes, the nitrocellulose membrane was vacuum-baked and the nylon membrane was UV cross-linked to immobilize the retained aptamers. The membranes were processed for chemiluminescent detection using the Pierce biotinylated nucleic acid detection kit following the manufacturer's instructions. The chemiluminescent signals were detected and imaged on a Chemimager (Alpha Innotech). Image analysis and quantification of spot intensities were conducted using ImageJ (version 1.43) (*37*). For binding analysis on nitrocellulose, background spot intensity due to buffer effect was subtracted from all data points and saturation binding curves were generated by curve fits assuming a single binding site. In the case of HABD, data from protein-dependent TA depletion on the nylon membrane were considered for analysis. The nylon spot intensity in the absence of protein was considered as the total amount of TA present. The depleted spot intensities due to protein binding for each protein concentration were calculated by subtraction from the intensity corresponding to the total amount of TA present. To confirm the specificity of the selected TAs for CD44−HABD, the selected TAs were tested for binding to another HA binding protein, HABP. This protein has the conserved Link module involving the HA binding site and shares 32.3% sequence identity with CD44 (*38*). Failure of the TAs to bind to HABP shows that the TA binding to CD44−HABD is not due to nonspecific electrostatic interactions.

```
TA1  primer-CCAAGGCCTGCAAGGGAACCAAGGACACAG-primer
TA2  primer-CCAAGGCATGCAAGGGAACCAAGGACACAG-primer
TA3  primer-TGCAGATGCAAGGTAACCATATCCAAAGCA-primer
TA4  primer-CGTATGCAAGGTGAAAGCAGCACACCAATA-primer
TA5  primer-GCGGCAGTAGTTGATCCCGAAGCGTTACGA-primer
TA6  primer-TTGGGACGGTGTTAAACGAAAGGGGACGAC-primer
```

FIGURE 1: Primary sequences of the thioaptamers selected after the 10th round of selection. Only the sequences of the variable, random region are shown. Sequences were aligned using ClustalW (*36*).

CD44 Immunostaining. The cells were grown on glass chamber slides, fixed with 4% paraformaldehyde for 10 min, and then washed with PBS buffer. The slides were incubated with protein block (10% normal goat serum in PBS) for 30 min and incubated with primary rat anti-mouse CD44 antibody (1:800 dilution, Abcam) at room temperature for 1 h. The same amount of affinity-purified normal IgG from the corresponding species was used as a negative control. The slides were washed and incubated with secondary goat anti-rat Alexa 568 IgG (1:400 dilution) for 30 min at room temperature in the dark. The slides were then washed with PBS and rinsed with deionized water. Nuclear counterstaining was performed with Hoechst 33342 (Sigma) for 5 min at room temperature. The images were acquired under the same condition using fluorescence microscopy (TE2000-E, Nikon) and processed by using Nikon Elements. Five randomly selected high-power fields at 60× magnification were shown.

Cell Binding Assay. CD44+ ovarian cancer cell lines (SKOV3, IGROV, and A2780) and the CD44− NIH3T3 cell line were plated onto eight-well glass chamber slides to allow them to attach for 24 h. The cells were incubated with 50 nM fluorescein-labeled TAs for 10 min at 37 °C. The slides were immediately washed with ice-cold PBS, and nuclei were counterstained with Hoechst 33342 (Sigma) for 5 min at room temperature. Series of images were obtained under the same conditions when fluorescence intensities needed to be compared.

RESULTS

Sequences of Selected Thioaptamers. After 10 rounds of selection using a combinatorial library containing potentially 10^{14} different sequences, the TA library converged to several sequence families. On the basis of the primary sequence alignments determined with ClustalW (*36*), the TA sequences were categorized into six groups (TA1−TA6). The variable region of the selected sequences is shown in Figure 1. The TGCAAGG(G/T)AACCA motif was found to occur in four of the six groups. Primary sequences of TA1 and TA2 differ by only one base.

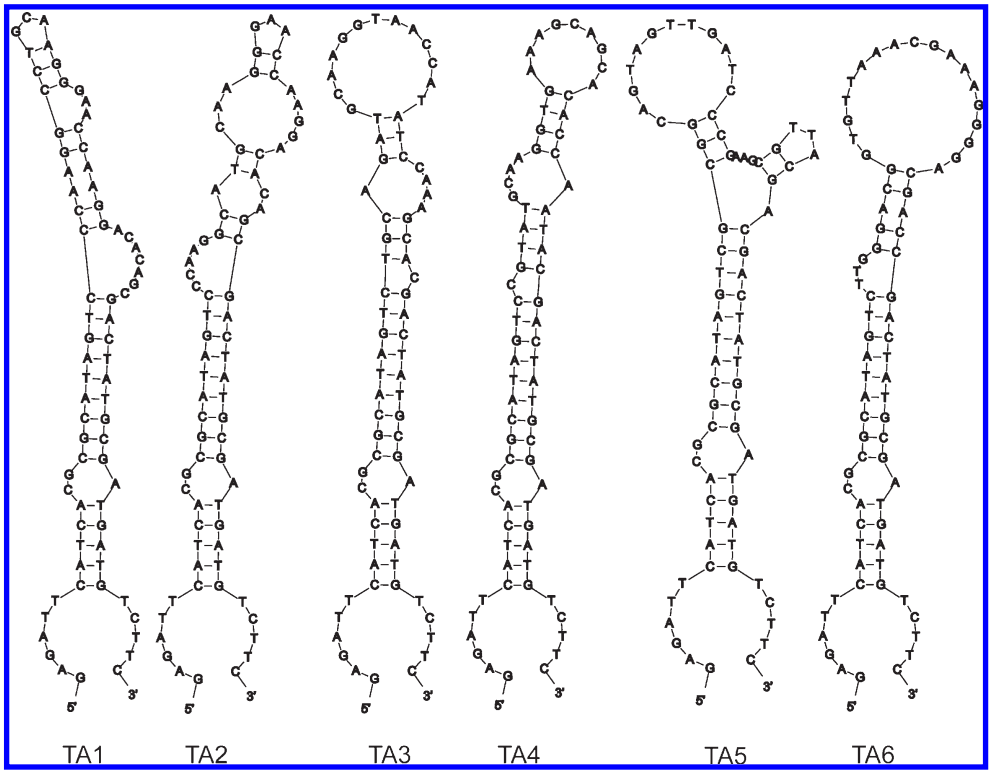

FIGURE 2: Secondary structures of the six thioaptamers. Secondary structures were predicted with MFold (*39*).

Because only dATP (αS) was used in the polymerization steps, all adenosines in the selected sequences beyond position 22 have a 5′-monothiophosphate substitution. MFold (*39*) (http://mfold.bioinfo.rpi.edu)-predicted secondary structures indicated that all six selected TA sequences can form hairpin loop structures with the random region forming the loop and the primer regions making up the stem regions (Figure 2).

Specific Binding of Selected Thioaptamers to CD44+ Cells. To test the selective binding of TAs to CD44, fluorescently tagged TAs (50 nM) were incubated with both CD44+ ovarian cancer cell lines (SKOV3, IGROV, and A2780) (*39*) and the CD44− NIH3T3 cell line for 10 min at 37 °C. The fluorescence intensities and localization were compared using a fluorescence microscope. TA1 and TA6 demonstrated rapid binding to the cell membranes of all CD44+ ovarian cancer cell lines at a concentration of 50 nM (Figure 3), whereas TA2 and TA3 showed weaker binding to the CD44+ cells. TA4 and TA5 did not show any binding to the CD44+ cells. In sharp contrast to the TA binding to CD44+ cells, none of TAs bound to CD44− NIH3T3 cells (Figure 3). Among five TA sequences, TA1 showed the strongest binding to the CD44+ ovarian cancer cells tested. This is supported by the large number of occurrences of TA1 sequences within the set of cloned sequences in the final selection round (data not shown). TAs were found in punctate structures at the membrane, which coincides with known CD44 surface expression patterns (*40*).

Binding of Selected Thioaptamers to CD44−HABD and CD44−Fc. Filter binding methods were used to quantitatively measure the binding of the selected TAs to the CD44. We used two constructs for this purpose, the HABD and CD44−Fc proteins. Filter binding assays were performed with the three TAs that showed binding to the CD44+ cells. All three TAs, TA1, TA3, and T6, showed binding to CD44−HABD. Only TA3 and TA6 showed binding to CD44−Fc. TA1 did not show binding to CD44−Fc. The saturation binding curves are shown in Figure 4. The equilibrium dissociation constants, K_d, were derived from these curves and are listed in Table 1. All TAs tested exhibited a nanomolar range of binding constants for the CD44 proteins (180−285 nM). The binding affinities (nanomolar) of the CD44 TAs are significantly better than that of HA [K_d = 61 μM (*6*)]. TA6 bound to CD44−HABD and CD44−Fc with the same affinity, while TA3 exhibited higher binding affinity for CD44−Fc. Both TA3 and TA6 showed similar binding constants with CD44−Fc. TA1 did not show any detectable binding to CD44−Fc. To confirm the specificity of our TAs with respect to CD44, we tested the binding of a random, 73-mer monothio-substituted oligonucleotide to CD44. This random oligonucleotide failed to bind to both recombinant CD44−HABD and CD44−Fc. All three TAs failed to bind to another HA binding protein, HABP. Both these results confirm that the selected TAs are specific for CD44−HABD.

DISCUSSION

In this study, we have selected TAs that specifically bind to the CD44's HABD with the goal of using these TAs for targeted delivery of therapeutic drugs to cancer cells expressing CD44. Targeted delivery of anticancer drugs specifically to the cancer cells will greatly enhance the efficacy and reduce adverse effects. Because CD44 is a membrane protein that is overexpressed on the plasma membrane of cancer cells and internalized into the cells upon ligand binding, CD44-targeted delivery presents a powerful strategy for selective cancer cell targeting. Because the HABD is highly conserved among all the splicing variants and all splicing variants contain the HABD in their extracellular domain, TAs specific for the HABD are valuable tools for recognizing cancer cells that express CD44 splicing variants.

Previous studies have reported using HA for selective targeting of cancer cells expressing CD44. HA-bound liposomes were used to deliver encapsulated doxorubicin to tumor cells expressing

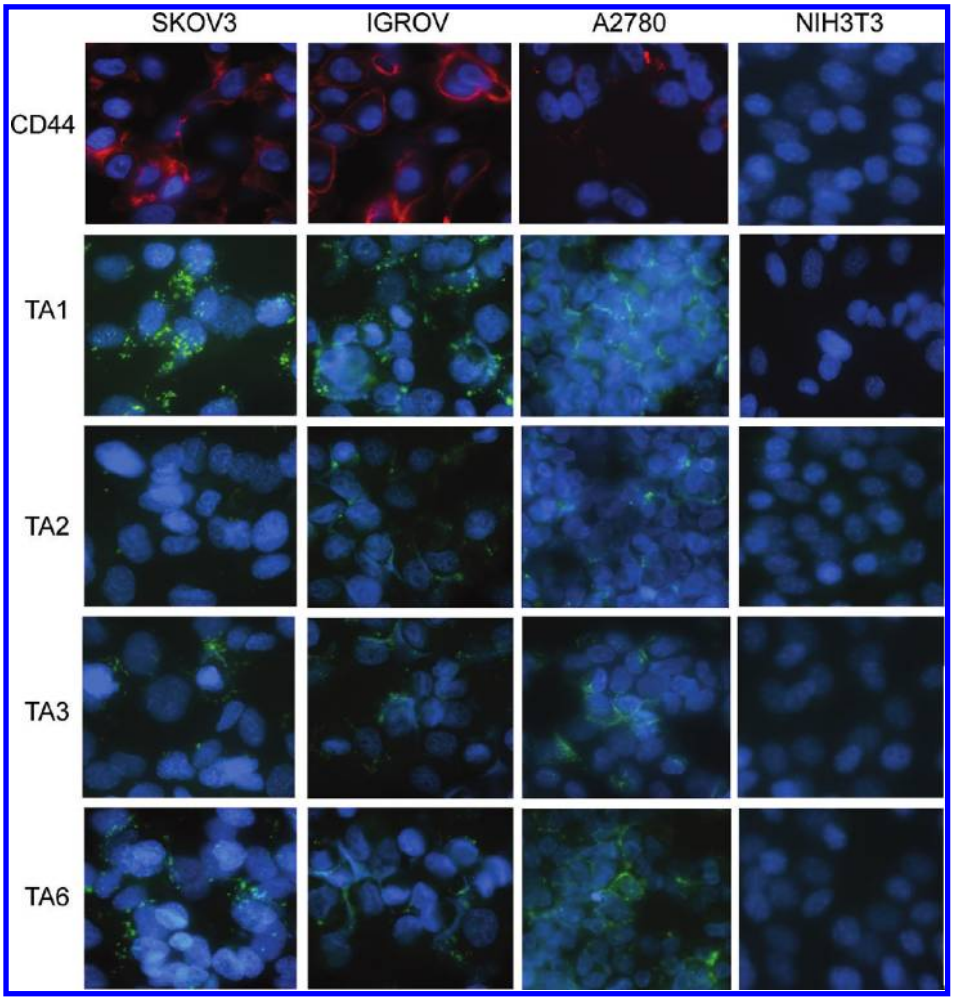

FIGURE 3: TA binding to CD44+ cells. CD44+ ovarian cancer cell lines (SKOV3, IGROV, and A2780) and the CD44 negative NIH3T3 cell line were incubated with 50 nM fluorescein-labeled TAs for 10 min at 37 °C. The slides were counterstained with Hoechst 33342 (green for fluorescein-labeled CD44 TA, blue for nuclear counterstaining, and red for CD44).

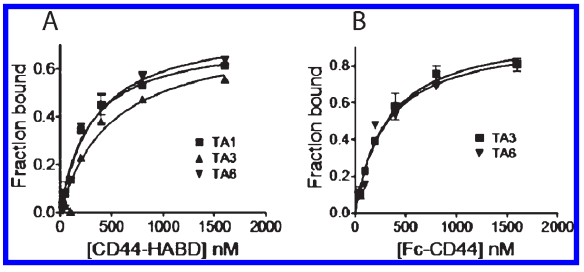

FIGURE 4: Saturation binding curves for binding of thioaptamers to CD44. Biotinylated thioaptamers were used in the assays. (A) Binding curves for CD44−Fc protein. The chemiluminescent spot intensities on the nitrocellulose membrane, due to retention of thioaptamers, are plotted as a function of total CD44−Fc protein concentration. (B) Binding curves for CD44−HABD. The chemilumniscent spot intensities on the nylon membrane, due to depletion of thioaptamers, are plotted as a function of total CD44−HABD concentration.

high levels of CD44 (*41*). However, there are several limitations in using HA for targeted delivery. HA is naturally present in the human body and can bind to several proteins besides CD44 (*42*), leading to nonspecific binding to other proteins. Our TAs showed specific binding to CD44 and failed to bind to another HA binding protein, HABP. HA is a large polymer and difficult to synthesize compared to oligonucleotides. Furthermore, several studies have reported that interactions of HA with the CD44 splice variants are weakened compared to those with CD44S (*20*).

Table 1: Equilibrium Dissociation Constants (nanomolar) of Selected Thioaptamers toward CD44−Fc and CD44−HABD[a]

thioaptamer	CD44−HABD	CD44−Fc
TA1	190.6 ± 25.4	
TA3	285.4 ± 83.1	188.1 ± 26.8
TA6	187.0 ± 30.6	179.4 ± 60.8

[a]The dissociation constants were derived from saturation binding curves shown in Figure 4. Binding experiments were performed at room temperature and pH 7.4.

The binding constants for the selected TAs reported in this study are significantly lower compared to the binding constants for binding of HA to CD44. Because TAs exhibit higher affinity and specificity than the HA, TAs would be a better ligand of HABD for achieving a higher level of refined targeting.

HA is known to regulate tumor progression through different mechanisms. Several studies have shown that HA binding activates CD44 and stimulates tumor progression (*11*, *43*, *44*). HA in its very large, high-molecular weight form is part of the extracellular matrix and is reported to promote cancer initiation and progression by activating signaling pathways and host−tumor interactions (*45*, *46*). Because the TAs are selected against the HABD of CD44, binding of the TAs would disrupt any further binding of HA to CD44 and could potentially interfere with tumor progression that depends on the HA binding-mediated

activation of CD44. While the high-molecular weight forms of HA have been shown to promote tumor progression, the small, low-molecular weight forms of HA have been shown to suppress tumor progression (*47*). The TAs are similar to the low-molecular weight forms of the HA and, therefore, might not trigger the same signaling pathways as the high-molecular weight HAs and promote tumor progression. Furthermore, binding of small HA oligomers to the surface of CD44 appears to enhance HA uptake (*48*). The selected TAs, being small oligonucleotides, might increase the level of internalization upon binding to CD44. TAs have several advantages over unmodified oligonucleotide aptamers. Thio-modified oligonucleotides exhibit a higher level of resistance to digestion by cellular nucleases (*28*, *29*). TAs also exhibit tighter binding toward target proteins compared to unmodified aptamers (*30*, *49*). It appears that the thiophosphates do not bind sodium ions as effectively as the unmodified phosphates, and thus, the thio-substituted phosphate esters act as nearly bare anions (*50*). Because less energy is required to strip the cations from the backbone of thio-substituted oligonucleotides, these agents can in principle bind more tightly to proteins. However, complete thio substitution of oligonucleotides could lead to nonspecific binding to other cellular proteins (*31*). Therefore, to achieve selective, high-affinity binding, optimization of the number of thio substitutions is critical. Our combinatorial selection methods allow us to select TAs with hybrid backbones in which the number and the position of the sulfur substitutions are optimized. This approach allows us to simultaneously select for both the sequence and the best monothiophosphate substitutions. In contrast, almost all modified aptamers are first selected by SELEX and then modified postselection. As we have shown previously (*49*−*51*), monothiophosphate substitutions can perturb both the structure and interaction with the target, and therefore, it is better to select both sequence modifications simultaneously. While the TAs selected showed specific binding to CD44, unmodified oligonucleotides containing the same primary sequences failed to bind to the CD44 proteins or to the CD44+ cells (data not shown). This observation shows that sulfur substitution at specific positions of the oligonucleotides led to specificity and higher-affinity binding to CD44.

We have used recombinant CD44−HABD for the iterative selection cycles. For membrane binding assays, we have used both the CD44−Fc chimera and CD44−HABD recombinant protein. It has been shown that CD44−HABD (residues 20−178) and the CD44−Fc chimera are structurally similar and share a common tertiary fold. On the basis of the similar reactivity of CD44−HABD and CD44−Fc toward the conformation sensitive mAbs BRIC-235 and F10.44.2, Teriete et al. (*52*) showed these two constructs are structurally similar. The concentration-dependent binding of HA to CD44−Fc is very similar to that of CD44−HABD. Our data demonstrated that TAs selected against CD44−HABD bound to both CD44−HABD and CD44−Fc with similar dissociation constants, supporting the notion of bioequivalence between these two protein constructs.

All TAs exhibited rapid and selective binding to cultured CD44+ cells, but not to the CD44− cells. Although preincubation of the CD44+ cells with HA (1 mM, 10 kDa) failed to block the binding of CD44 TA (data not shown), it does not preclude the HABD selective binding of CD44 TA because there are substantial differences in the binding affinities for binding of TA and HA to CD44. We identified TAs that bind to CD44−HABD with nanomolar affinity, binding significantly stronger than that of its natural ligand HA, and will be of great interest for further development as a targeting or imaging agent for the delivery of therapeutic payloads to cancer tissues.

ACKNOWLEDGMENT

We thank Dr. Anil Sood of the University of Texas M. D. Anderson Cancer Center for the gift of CD44 positive cancer cell lines used in this study and Dr. David Volk of the University of Texas Health Science Center for helpful discussions.

REFERENCES

1. Naor, D., Sionov, R. V., and Ish-Shalom, D. (1997) CD44: Structure, function, and association with the malignant process. *Adv. Cancer Res. 71*, 241–319.
2. Strobel, T., Swanson, L., and Cannistra, S. A. (1997) In vivo inhibition of CD44 limits intra-abdominal spread of a human ovarian cancer xenograft in nude mice: A novel role for CD44 in the process of peritoneal implantation. *Cancer Res. 57*, 1228–1232.
3. Wallach-Dayan, S. B., Rubinstein, A. M., Hand, C., Breuer, R., and Naor, D. (2008) DNA vaccination with CD44 variant isoform reduces mammary tumor local growth and lung metastasis. *Mol. Cancer Ther. 7*, 1615–1623.
4. Kohda, D., Morton, C. J., Parkar, A. A., Hatanaka, H., Inagaki, F. M., Campbell, I. D., and Day, A. J. (1996) Solution structure of the Link module: A hyaluronan-binding domain involved in extracellular matrix stability and cell migration. *Cell 86*, 767–775.
5. Banerji, S., Ni, J., Wang, S. X., Clasper, S., Su, J., Tammi, R., Jones, M., and Jackson, D. G. (1999) LYVE-1, a new homologue of the CD44 glycoprotein, is a lymph-specific receptor for hyaluronan. *J. Cell Biol. 144*, 789–801.
6. Banerji, S., Wright, A. J., Noble, M., Mahoney, D. J., Campbell, I. D., Day, A. J., and Jackson, D. G. (2007) Structures of the CD44-hyaluronan complex provide insight into a fundamental carbohydrate-protein interaction. *Nat. Struct. Mol. Biol. 14*, 234–239.
7. Takeda, M., Ogino, S., Umemoto, R., Sakakura, M., Kajiwara, H., Sugahara, K. N., Hayasaka, H., Miyasaka, M., and Shimada, I. (2006) Ligand-induced structural changes of the CD44 hyaluronan-binding domain revealed by NMR. *J. Biol. Chem. 281*, 40089–40095.
8. Ogino, S., Nishida, N., Umemoto, R., Suzuki, M., Takeda, M., Terasawa, H., Kitayama, J., Matsumoto, M., Hayasaka, H., Miyasaka, M., and Shimada, I. (2010) Two-state conformations in the hyaluronan-binding domain regulate CD44 adhesiveness under flow condition. *Structure 18*, 649–656.
9. Skotheim, R. I., and Nees, M. (2007) Alternative splicing in cancer: Noise, functional, or systematic? *Int. J. Biochem. Cell Biol. 39*, 1432–1449.
10. Afify, A., Pang, L., and Howell, L. (2007) Diagnostic utility of CD44 standard, CD44v6, and CD44v3-10 expression in adenocarcinomas presenting in serous fluids. *Appl. Immunohistochem. Mol. Morphol. 15*, 446–450.
11. Bourguignon, L. Y. W., Singleton, P., Zhu, H., and Zhou, B. (2002) Hyaluronan (HA) promotes signaling interaction between CD44 and the TGF-RI receptor in metastatic breast tumor cells. *J. Biol. Chem. 277*, 39703–39712.
12. An, Y., and Ongkeko, W. M. (2009) ABCG2: The key to chemoresistance in cancer stem cells? *Expert Opin. Drug Metab. Toxicol. 5*, 1529–1542.
13. Mani, S. A., Guo, W., Liao, M. J., Eaton, E. N., Ayyanan, A., Zhou, A. Y., Brooks, M., Reinhard, F., Zhang, C. C., Shipitsin, M., Campbell, L. L., Polyak, K., Brisken, C., Yang, J., and Weinberg, R. A. (2008) The epithelial-mesenchymal transition generates cells with properties of stem cells. *Cell 133*, 704–715.
14. Toole, B. P., and Slomiany, M. G. (2008) Hyaluronan, CD44 and Emmprin: Partners in cancer cell chemoresistance. *Drug Resist. Updates 11*, 110–121.
15. Alvero, A. B., Chen, R., Fu, H. H., Montagna, M., Schwartz, P. E., Rutherford, T., Silasi, D. A., Steffensen, K. D., Waldstrom, M., Visintin, I., and Mor, G. (2009) Molecular phenotyping of human ovarian cancer stem cells unravels the mechanisms for repair and chemoresistance. *Cell Cycle 8*, 158–166.
16. Hu, L., McArthur, C., and Jaffe, R. B. (2010) Ovarian cancer stem-like side-population cells are tumourigenic and chemoresistant. *Br. J. Cancer 13*, 1276–1283.
17. Fong, M. Y., and Kakar, S. S. (2010) The role of cancer stem cells and the side population in epithelial ovarian cancer. *Histol. Histopathol. 25*, 113–120.

18. Peer, D., and Margalit, R. (2004) Tumor-targeted hyaluronan nanoliposomes increase the antitumor activity of liposomal Doxorubicin in syngeneic and human xenograft mouse tumor models. *Neoplasia 6*, 343–353.
19. Auzenne, E., Ghosh, S. C., Khodadadian, M., Rivera, B., Farquhar, D., Price, R. E., Ravoori, M., Kundra, V., Freedman, R. S., and Klostergaard, J. (2007) Hyaluronic acid-paclitaxel: Antitumor efficacy against CD44(+) human ovarian carcinoma xenografts. *Neoplasia 9*, 479–486.
20. Jackson, D. G., Bell, J. I., Dickinson, R., Timans, J., and Whittle, J. N. (1995) Proteoglycan forms of the lymphocyte homing receptor CD44 are alternatively spliced variants containing the v3 exon. *J. Cell Biol. 128*, 673–685.
21. Gold, L. (1995) Oligonucleotides as research, diagnostic and therapeutic agents. *J. Biol. Chem. 270*, 13581–13584.
22. Thiviyanathan, V., Somasunderam, A. D., and Gorenstein, D. G. (2007) Combinatorial selection and delivery of thioaptamers. *Biochem. Soc. Trans. 35*, 50–52.
23. Cho, E. J., Lee, J. W., and Ellington, A. D. (2009) Applications of aptamers as sensors. *Annu. Rev. Anal. Chem. 2*, 241–264.
24. Keefe, A. D., Pai, S., and Ellington, A. (2010) Aptamers as therapeutics. *Nat. Rev. 9*, 537–550.
25. Tuerk, C., and Gold, L. (1990) Systematic evolution of ligands by exponential enrichment: RNA ligands to bacteriophage T4 DNA polymerase. *Science 249*, 505–510.
26. Ellington, A. D., and Szostak, J. W. (1990) In vitro selection of RNA molecules that bind specific ligands. *Nature 346*, 818–822.
27. Luzi, E., Minunni, S., Tombelli, S., and Mascini, M. (2003) New trends in affinity sensing: Aptamers for ligand binding. *Trends Anal. Chem. 22*, 810–818.
28. Jhaveri, S., Olwin, B., and Ellington, A. D. (1998) In vitro selection of phosphorothiolated aptamers. *Bioorg. Med. Chem. Lett. 8*, 2285–2290.
29. Micklefield, J. (2001) Backbone modification of nucleic acids: Synthesis, structure and theraputic applications. *Curr. Med. Chem. 8*, 1157–1179.
30. Milligan, J. F., and Uhlenbeck, O. C. (1989) Determination of RNA-protein contacts using thiophosphate substitutions. *Biochemistry 28*, 2849–2855.
31. King, D. J., Bassett, S. E., Li, X., Fennewald, S. A., Herzog, N. K., Luxon, B. A., Shope, R., and Gorenstein, D. G. (2002) Combinatorial selection and binding of phosphorothioate aptamers targeting human NF-κB RelA(p65) and p50. *Biochemistry 41*, 9696–9706.
32. King, D. J., Ventura, D. A., Brasier, A. R., and Gorenstein, D. G. (1998) Novel combinatorial selection of phosphorothioate oligonucleotide aptamers. *Biochemistry 37*, 16489–16493.
33. Somasunderam, A., Ferguson, M. R., Rojo, D. R., Thiviyanathan, V., Li, X., O'Brien, W. A., and Gorenstein, D. G. (2005) Combinatorial selection, inhibition and antiviral activity of DNA thioapatamers targeting the RNase H domain of HIV-1 reverse transcriptase. *Biochemistry 44*, 10388–10395.
34. Neerathilingam, M., Greene, L. H., Colebrooke, S. A., Campbell, I. D., and Staunton, D. (2005) Quantitation of protein expression in a cell-free system: Efficient detection of yields and ^{19}F NMR to identify folded protein. *J. Biomol. NMR 31*, 11–19.
35. Banerji, S., Day, A. J., Kahmann, J. D., and Jackson, D. G. (1998) Characterization of a functional hyaluronan-binding domain from the human CD44 molecule expressed in *Escherichia coli*. *Protein Expression Purif. 14*, 371–381.
36. Thompson, J. D., Higgins, D. G., and Gibson, T. J. (1994) CLUSTALW: Improving the sensitivity of progressive multiple sequence alignment through sequence weighting, position-specific gap penalties and weight matrix choice. *Nucleic Acids Res. 22*, 4673–4680.
37. Abramoff, M. D., Magelhaes, P. J., and Ram, S. J. (2004) Image processing with ImageJ. *Biophotonics Intl. 11*, 36–42.
38. Kohda, D., Morton, C. J., Parker, A. A., Inagaki, F. M., Campbell, I. D., and Day, A. J. (1996) Solution Structure of the Link Module: A Hyaluronan-binding domain involved in extracellular matrix stability and cell migration. *Cell 86*, 767–775.
39. Zuker, M. (2003) Mfold web server for nucleic acid folding and hybridization prediction. *Nucleic Acids Res. 31*, 3406–3415.
40. Chen, H., Hao, J., Wang, L., and Li, Y. (2009) Co-expression of invasive markers (uPA, CD44) and multiple drug-resistance proteins (MDR1, MRP2) is correlated with epithelial ovarian cancer progression. *Br. J. Cancer 101*, 432–440.
41. Eliaz, R. E., and Szoka, F. C. (2001) Liposome-encapsulated Doxyrubicin targeted to CD44. *Cancer Res. 61*, 2592–2601.
42. Yokoo, M., Miyahayashi, Y., Naganuma, T., Kimura, N., Sasada, H., and Sato, E. (2002) Identification of hyaluronic acid-binding proteins and their expressions in porcine cumulusoocyte complexes during in vitro maturation. *Biol. Reprod. 67*, 1165–1171.
43. Heldin, P., Karousou, E., Bernert, B., Porsch, H., Nishitsuka, K., and Skandalia, S. S. (2008) Importance of Hyaluronan-CD44 interactions in inflammation and tumorigenesis. *Connect. Tissue Res. 49*, 215–218.
44. Turley, E. A., Nobel, P. W., and Bourguignon, L. Y. W. (2002) Signaling properties of hyaluronan receptors. *J. Biol. Chem. 277*, 4589–4592.
45. Itano, N., Zhuo, L., and Kimata, K. (2008) Impact of the hyaluronan-rich tumor microenvironment on cancer initiation and progression. *Cancer Sci. 99*, 1720–1725.
46. Misra, S., Hascall, V. C., Berger, F. G., Markwalk, R. R., and Ghatak, S. (2008) Hyaluronan, CD44 and cyclooxygenase-2 in colon cancer. *Connect. Tissue Res. 49*, 219–224.
47. Alaniz, L., Rizzo, M., Malvicini, M., Jaunarena, J., Avella, D., Atorrasagasti, C., Aquino, J. B., Garcia, M., Matar, P., Silva, M., and Mazzolini, G. (2009) Low molecular weight hyaluronan inhibits colorectal carcinoma growth by decreasing tumor cell proliferation and stimulating immune response. *Cancer Lett. 278*, 9–16.
48. Slomiany, M. G., Dai, L., Bomer, P. A., Knackstedt, T. J., Kranc, D. A., Tolliver, L., Maria, B. L., and Toole, B. P. (2009) Abrogating drug resistance in malignant peripheral nerve sheath tumors by disrupting hyaluronan-CD44 interactions with small hyaluronan oligosaccharides. *Cancer Res. 69*, 4992–4998.
49. Yang, X., and Gorenstein, D. G. (2004) Progress in thioaptamer development. *Curr. Drug Targets 5*, 705–715.
50. Volk, D. E., Power, T. D., Gorenstein, D. G., and Luxon, B. A. (2002) An ab initio study of phosphorothioate and phosphorodithioate interactions with sodium cation. *Tetrahedron Lett. 43*, 4443–4447.
51. Volk, D. E., Yang, X., Fennewald, S. M., King, D. J., Bassett, S. E., Venkitachalam, S., Herzog, N., Luxon, B. A., and Gorenstein, D. G. (2002) Solution structure and design of dithiophosphate backbone aptamers targeting transcription factor NF-κB. *Bioorg. Chem. 30*, 396–419.
52. Teriete, P., Banerji, S., Noble, M., Blundell, C. D., Wright, A. J., Pickford, A. R., Lowe, E., Mahoney, D. J., Tammi, M. I., Kahmann, J. D., Campbell, I. D., Day, A. J., and Jackson, D. G. (2004) Structure of the regulatory hyaluronan binding domain in the inflammatory leukocyte homing receptor CD44. *Mol. Cell 13*, 483–496.